

Applications of Bayesian Model Selection to Cosmological Parameters

Roberto Trotta[?]

Oxford University, Astrophysics, Denys Wilkinson Building, Keble Road, OX1 3RH, United Kingdom
D epartement de Physique Théorique, Université de Genève, 24 quai Ernest Ansermet, 1211 Genève 4, Switzerland

7 February 2020

ABSTRACT

Bayesian evidence is a tool for model comparison which can be used to decide whether the introduction of a new parameter is warranted by data. I show that the usual sampling statistic rejection tests for a null hypothesis can be misleading, since they do not take into account the information content of the data. I review the Laplace approximation and the Savage-Dickey density ratio to compute Bayes factors, which avoid the need of carrying out a computationally demanding multidimensional integration. I present a new procedure to forecast the Bayes factor of a future observation by computing the Expected Posterior Odds (ExPO). As an illustration, I consider three key parameters for our understanding of the cosmological concordance model: the spectral tilt of scalar perturbations, the spatial curvature of the Universe and a CDM isocurvature component to the initial conditions which is totally (anti)correlated with the adiabatic mode. I find that current data are not informative enough to draw a conclusion on the status of the spectral tilt, while there is moderate evidence for a flat Universe (with odds of order 10 : 1) and strong evidence for purely adiabatic initial conditions (odds larger than 1000 : 1). I show that the Planck satellite has about 90% of probability of gathering large evidence against a scale invariant spectral index, while a clear cut model selection for a flat universe will still require the use of data complementary to CMB measurements. The issue of priors in Bayesian model selection is also discussed, and it is shown that in a phenomenological modelling the prior for a given experiment can be computed by sensitivity analysis.

Key words: Cosmology { Bayesian evidence { Model comparison { Spectral index { Flatness { Isocurvature modes

1 INTRODUCTION

In the epoch of precision cosmology, we often face the problem of deciding whether or not cosmological data support the introduction of a new quantity in our model. For instance, we might ask whether it is necessary to consider a running of the spectral index, an extra isocurvature mode, or a non-constant dark energy equation of state. This kind of questions should be considered in the framework of model selection, rather than as a parameter estimation problem. In fact, the inference step of parameter estimation assumes the underlying model to be true. In order to question this assumption, and determine what the data have to say about it, we must instead take the standpoint of a model selection approach.

The key quantity for Bayesian model comparison is the evidence. Promoted by the recent revival of Bayesian meth-

ods in cosmology, the issue of computing and interpreting the evidence is attracting increasing attention. Recent works have focused on the isocurvature contribution to primordial perturbations (Beltran et al. 2005), the dark energy equation of state (Saini et al. 2004; Bassett et al. 2004), a specific implementation of the curvaton scenario (Lazarides et al. 2004), a consistency check between data-sets (Hobson et al. 2002; Marshall et al. 2004). Perhaps the most relevant application bears on the number of cosmological parameters. It is generally agreed that a core of 6 parameters (supplemented by a bias parameter) is sufficient to describe and in reasonable agreement with most of current cosmological observations, see e.g. Tegmark et al. (2004b). These parameters are the baryon, the cold dark matter and cosmological constant densities, the Hubble parameter, the optical depth to reionization, the scalar spectral index and the amplitude of the primordial (adiabatic) density fluctuations. The status of additional parameters is less certain, as often constraints on their value do not allow to rule them out on the basis

[?] E-mail address: rxt@astro.ox.ac.uk

2 Roberto Trotta

of sampling statistics rejection tests. The purpose of this work is to clarify the role of Bayesian model comparison in answering such questions, and highlight the difference with the usual criteria for null hypothesis testing.

This paper is organized as follows: in section 2, we briefly review Bayesian inference and model comparison and compare this approach with sampling statistics hypothesis testing. We give an illustration of Lindley's paradox, showing that sampling statistics can yield misleading results because it ignores the information content of the data. Section 3 introduces the Laplace approximations and the Savage-Dickey density ratio for the computation of evidence ratios (Bayes factor), and presents a new method to forecast the Bayes factor of a future observation, called ExPO (for 'Expected Posterior Odds'). Section 4 is devoted to the application of those tools to three central parameters of the cosmological concordance model: the spectral tilt of scalar perturbations, the spatial curvature of the Universe and a totally (anti)correlated isocurvature CDM contribution to the initial conditions. We discuss our results in Section 5 and summarize our conclusions in Section 6.

2 BAYESIAN INFERENCE

This section briefly reviews some concepts of Bayesian statistics and introduces the notation used throughout this work. We also argue for the need of Bayesian model comparison by illustrating Lindley's paradox with a toy example.

2.1 Bayesian parameter estimation

Bayesian inference is based on Bayes' theorem, which is nothing more than a straightforward consequence of the product rule of probability theory:

$$P(A|B) = \frac{P(B|A)P(A)}{P(B)} \quad (\text{Bayes' theorem}). \quad (1)$$

Here A, B denote two propositions, P represents the probability assignment and the vertical bar designates that the proposition on its right is assumed true. In order to clarify the meaning of this relation, let us write (\cdot) a vector of d parameters under a model M for A and D (the data at hand) for B , obtaining

$$\begin{aligned} P(\mathcal{D};M) &= \frac{P(L(D_j;M) | (\cdot);M)}{P(L(D_j;M) | (\cdot);M)d} \\ &= \frac{L(D_j;M) | (\cdot);M}{P(L(D_j;M))}, \end{aligned} \quad (2)$$

where (\cdot) designates the parameter space (of dimensionality d) under model M . This equation relates the posterior probability $P(\mathcal{D};M)$ for the parameters of the model M given the data D to the likelihood function $L(D_j;M)$ if the prior probability distribution function $(\cdot;M)$ for the parameters under the model is known. The latter is called 'prior' for short. The quantity in the denominator is independent of (\cdot) and is called the evidence of the data for the model M (see e.g. Mackay (2003)). The evidence is the central quantity for model comparison, as we shall see, but, in the context of parameter estimation within a model, it is just

an overall multiplicative constant which does not matter. In short,

$$\text{posterior} = \frac{\text{likelihood} \cdot \text{prior}}{\text{evidence}}: \quad (3)$$

The prior distribution contains all the knowledge about the parameters before observing the data, i.e. our physical understanding of the model, our insight into the experimental setup and its performance, and in short all our prior scientific experience. This information is then updated via Bayes' theorem to the posterior distribution by multiplying the prior with the likelihood function which contains the information coming from the data. The posterior probability is the base for inference about M . Within a given model M , the most probable value for the parameters is the one for which the posterior probability is largest.

Bayes' postulate states that, in the absence of other arguments, the prior probability should be assumed to be equal for all values of the parameters over a certain range ($m_{\min} \dots m_{\max}$). This is called a 'flat prior', i.e.

$$(\cdot;M) = [(\cdot; m_{\min}) \dots (\cdot; m_{\max})] \prod_{j=1}^d \frac{1}{m_{\max} - m_{\min}}, \quad (4)$$

where Θ is the Heaviside step function and $m_{\min} < j < m_{\max}$. Clearly, a flat prior does not correspond to a flat prior on some other set (\cdot) obtained via a non-linear transformation, since the two prior distributions are related via

$$(\cdot;M) = (\cdot;M) \frac{d(\cdot)}{d}: \quad (5)$$

A recurrent criticism is that the final inference depends on the prior which one chooses to use. However, for informative data the posterior is effectively dominated by the likelihood, and the choice of prior will not matter much. Conversely, if the inference strongly depends on the prior distribution, then this should be interpreted as a warning, telling us that the data are not powerful enough to clearly single out the parameter under consideration.

2.2 Bayesian model comparison

Let us move one step further. Consider two competing models M_0 and M_1 and ask what is the posterior probability of each model given the data D . By Bayes' theorem we have

$$P(M_i|\mathcal{D}) / P(M_j|\mathcal{D}) \quad (i=0,1); \quad (6)$$

where $P(D|M_i)$ is the evidence of the data under model M_i and (M_i) is the prior probability of the i th model before we see the data. The ratio of the posterior probabilities for the two competing models is called Bayes factor:

$$B_{01} = \frac{P(M_0|\mathcal{D})}{P(M_1|\mathcal{D})}: \quad (7)$$

Usually, we do not hold any prior beliefs about the two models and therefore $(M_0) = (M_1) = 1/2$, so that the Bayes factor reduces to the ratio of the evidences. The Bayes factor can be interpreted as an automatic Occam's razor, which disfavors complex models involving many parameters (see e.g. Mackay (2003) for details). A Bayes factor $B_{01} > 1$ favors model M_0 and in terms of betting odds it would

prefer M_0 over M_1 with odds of B_{01} against 1. The converse is true for $B_{01} < 1$. It is usual to consider the logarithm of the Bayes factor, for which the rule of thumb is that a substantial (strong) preference for one of the competing models requires at least $\ln B_{01} \geq 1.2$ (> 2.3), see e.g. Kass & Raftery (1995).

The evidence in favor of M can be evaluated by performing the integral

$$\begin{aligned} P(D|M) &= \int L(D;j;M) \pi(j|M) dj \\ &= P(D|M)d; \end{aligned} \quad (8)$$

where $P(D|M)$ designates the non-normalized posterior probability (i.e. the numerator in the right hand side of Eq. (2)). Computing the above integral from the MC samples is difficult, since there will be very few or no samples in the tails of the likelihood. A brute force approach is thermodynamic integration (Beltran et al. (2005) and references therein), which however requires about 10^7 evaluations of the likelihood and is thus computationally intensive. An elegant algorithm to compute the evidence has been recently proposed by Skilling (2004). It is however of great interest to develop alternative methods which avoid altogether the computational burden of carrying out the multi-dimensional integration of Eq. (8) and which allow for a quicker estimation of the Bayes factor. In this paper, we explore the Laplace approximation, which relies on approximating the posterior with a Gaussian, and the Savage-Dickey density ratio, which for nested models is equivalent to thermodynamic integration but requires far less computational power (for other possibilities, see e.g. DiCiccio et al. 1997). But first let us motivate the necessity of a Bayesian model selection viewpoint in cosmology.

2.3 Lindley's paradox: the number of 's is not enough

In cosmology, one is often interested in deciding whether a certain parameter is different from a reference value expected under a given model. For instance, one might want to know whether the scalar spectral index n_s "significantly" deviates from the scale-invariant value, $n_s = 1$, or the spatial curvature is different from zero, or the isocurvature amplitude non-zero. In the terminology of orthodox (sampling) statistics, one would need to perform a rejection test for the null hypothesis $H_0 : ! = !_0$, against the alternative hypothesis $H_1 : ! \neq !_0$, for a reference value $!_0$.

In practice, one usually performs a (Bayesian) parameter estimation for $!$, determining for instance with Monte Carlo (MC) methods the posterior mean, $\hat{!}$, and standard deviation, $\hat{\sigma}$, of the parameter of interest. Then one quotes the distance of the estimated mean for the parameter from the reference value, in units of the estimated standard deviation,

$$\frac{\hat{!} - !_0}{\hat{\sigma}}: \quad (9)$$

This "number of sigma's" difference is interpreted as a measure of the confidence with which one can reject H_0 . As we show below, this reasoning can lead to conclusions in strong

disagreement with the Bayesian evaluation of the model evidence, i.e. a value $!_0$ rejected under a frequentist test can on the contrary be favored by Bayesian model comparison. This is the content of Lindley's paradox (Lindley 1957). To illustrate how it arises, we briefly introduce in the next subsection some precisions regarding the terminology used in sampling statistics, then we show in 2.3.2 that the Bayes factor is consistent with our intuition of "Occam's razor" because it does take into account the "information content" of the data, ignored in sampling statistics.

2.3.1 Sampling statistics hypothesis testing

Consider the following elementary illustration: take n independent measurements x_1, x_2, \dots, x_n of the quantity x , which (from a sampling theory point of view, see Jaynes (2003, Chap. 16)) are drawn from a Gaussian sampling distribution with known variance, σ^2 . A sufficient estimator for the population mean, $!$, is the sample mean,

$$\hat{!} = \frac{1}{n} \sum_{j=1}^n x_j; \quad (10)$$

and its sampling distribution is

$$N(\hat{!}; \sigma^2/n) \quad (11)$$

where $N(\hat{!}; \sigma^2/n)$ denotes a Gaussian distribution with mean and standard deviation σ/\sqrt{n} . In this formulation the data are drawn from a population with certain statistical characteristics (i.e., if we were to repeat the drawing of the n samples a large number of times, then the relative frequency of generation of the data would tend to a Gaussian distribution (this is a property of the data themselves). Now assume that we have measured $\hat{!} > !_0$, and we ask the question: "Assuming that our data come from a normal distributed population with mean $!_0$ and variance σ^2 , what is the probability that our estimator (i.e., the sample mean) took a value equal or larger than the actual measured value $\hat{!}$ (if we repeated the measurement M 1 times)?". The answer is the p-value

$$p\text{-value} = P(\hat{!} \geq \hat{!}_0; \sigma^2/n) \quad (12)$$

which is then compared to a number α , called the "significance level" of the test. If $p\text{-value} < \alpha$, the hypothesis $H_0 : ! = !_0$ is rejected at the $1 - \alpha$ confidence level. This does not mean that the p-value is the probability of H_0 to be true, but rather that the p-value is the probability of falsely rejecting a true model H_0 (i.e., the probability that a rare event occurs when H_0 is true, or a Type I error).

Let us write for the measured sample mean

$$\hat{!} = !_0 + \hat{\sigma} Z_1 \quad (13)$$

with $\hat{\sigma} = \sigma/\sqrt{n}$ the estimated standard deviation after a fixed number of measurements n and Z_1 given in Eq. (9) a dimensionless number which indicates "how many sigma's away" is our estimate of the mean, $\hat{!}$, from its value under H_0 , $!_0$. If we pick a (fixed) confidence level, say $\alpha = 0.05$, then the frequentist significance test will reject the null hypothesis if

$$Z_1 \geq \frac{1}{2} \exp(-\hat{\sigma}^2/2) = 1.96 \quad (14)$$

(for a 2-tailed test). For $\sigma = 0.05$ the equality in Eq. (14) holds for $\omega_0 = 1.96$. In other words, sampling statistics reject the null hypothesis at the 95% confidence level if the measured mean is more than $\omega_0 = 1.96$ standard deviations away from the predicted ω_0 under H_0 .

2.3.2 Bayesian evidence and information content

Let us now turn to the Bayesian model comparison approach. The two competing models are M_0 with no free parameters, in which the value of ω is fixed to $\omega = \omega_0$, and model M_1 , with one free parameter $\omega \in [\omega_0, \infty)$. Under M_1 , our prior belief before seeing the data on the probability distribution of ω is explicitly represented by the 'prior pdf' $p(\omega; M_1) = p(\omega; M_0)$. This prior pdf is then updated to the posterior via Bayes theorem, Eq. (2). We thus interpret Eq. (11) as a function of the parameter ω for the observed data $\hat{\omega}$ and call it the likelihood function

$$L(\hat{\omega}; \omega) = p(\hat{\omega}; \omega). \quad (15)$$

Notice that, after applying Bayes theorem, the posterior probability is attached to the parameter ω itself, not to the estimator $\hat{\omega}$ as in sampling theory. In the Bayesian framework we only deal with observed data, never with properties of estimators based on a (factual) infinite replication of the data. In cosmology one only has one realization of the Universe and there is not even the conceptual possibility of reproducing the data ad infinitum and therefore the Bayesian standpoint seems better suited to such a situation.

Following Bayes postulate, we could take a flat prior on ω of the form (4) around ω_0 , of width σ

$$p(\omega) = [(\omega - \omega_0 + \sigma/2) (\omega_0 + \sigma/2 - \omega)] = \frac{1}{\sigma}, \quad (16)$$

but we will actually see that the details of the prior distribution do not matter in the informative case. The Bayes factor B_{01} in favor of model M_0 is, from Eq. (7),

$$B_{01} = \frac{1}{2} \exp \left(\frac{(\hat{\omega} - \omega_0)^2}{2\sigma^2} \right) \quad (17)$$

$$Z = \frac{(\hat{\omega} - \omega_0) + \sigma/2}{\sigma} \quad Z = \frac{(\hat{\omega} - \omega_0) - \sigma/2}{\sigma} = \frac{1}{\sigma};$$

where the function $Z(y)$ is defined in (14). The Z term is a consequence of the top-hat prior, which cuts sharply the posterior and introduces those corrections in the computation of the normalizing constant. Let us introduce $\hat{\omega} = \omega$, representing the factor by which the accessible parameter space under M_1 is reduced after the arrival of the data. Then in terms of ω , defined in Eq. (9), and σ , we have

$$B_{01}(\omega; \sigma) = \frac{1}{2} \exp \left(\frac{(\hat{\omega} - \omega)^2}{2\sigma^2} \right) \quad (18)$$

$$Z = \frac{1}{2} \quad Z = + \frac{1}{2} = \frac{1}{\sigma};$$

For $\hat{\omega} = \omega_0$, the posterior is well localized within the boundaries of the prior and the term in square brackets in (18) tends to 1.

Another simple choice for the prior is a Gaussian centered on ω_0 of standard deviation $\sigma/2$, which we denote by $N(\omega_0; \sigma/2)$, and the factor 1/2 is chosen to simplify

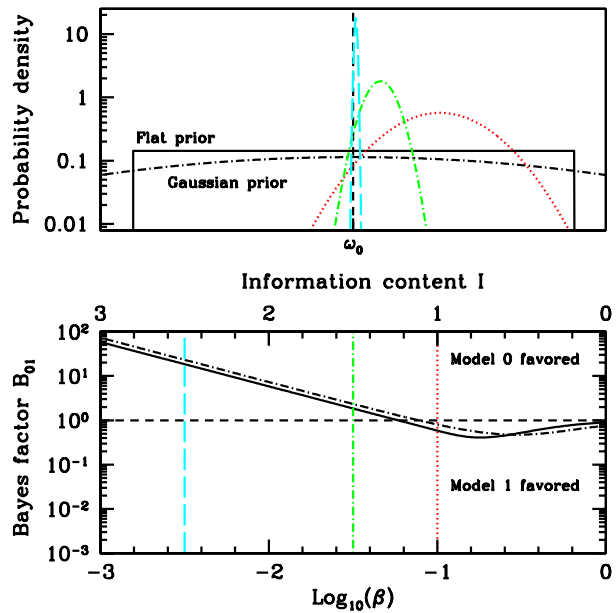


Figure 1. Illustration of Lindley's paradox. Sampling statistics hypothesis testing rejects the hypothesis that $\omega = \omega_0$ with 95% confidence in all 3 cases (color curves) illustrated in the top panel ($\sigma = 1.96$ in all cases). Bayesian evidence does take into account the information content of the data I , and correctly favors the simpler model (predicting that $\omega = \omega_0$) for informative data (left vertical line in the bottom panel, $I = 2.5$), with odds of 18 : 1 (for a flat prior, solid black line). Using a Gaussian prior (dashed-dotted black line) instead of a flat prior changes the result only very weakly.

the comparison with the flat prior case. With this choice of prior we obtain

$$B_{01}(\omega; \sigma) = \frac{1}{2} \exp \left(\frac{(\hat{\omega} - \omega)^2}{2(1 + 4^{-1})} \right) : \quad (19)$$

The Bayes factor thus depends not only on σ , but also on the quantity I , which is proportional to the volume occupied by the posterior in parameter space and describes the information gain in going from prior to posterior. A formal measure of information content is the Shannon entropy of the posterior pdf $P(\omega)$, defined as

$$S = - \int P(\omega) \ln P(\omega) : \quad (20)$$

For a Gaussian distribution, $P(\omega) = N(\omega; \sigma)$, Shannon entropy reduces to $S = \ln \sigma$, up to constant terms. While Shannon entropy is a more general measure, in order to reduce the computational burden we shall consider instead the information content of the data, I , simply defined as

$$I = \log_{10} \left(\frac{1}{\sigma} \right) = \log_{10} \left(\frac{1}{\hat{\omega} - \omega_0} \right); \quad (21)$$

The quantity I describes the order of magnitude by which our prior knowledge has improved after the arrival of the data. More informative data yield a smaller posterior spread and thus show a larger I . For a Gaussian posterior, I is equivalent to S up to a constant shift.

To highlight the role of the information content in the Bayesian context, imagine to perform three different measurements, with different values of I , i.e. with different in-

formation content I , but with outcomes such that \bar{x} is the same in all three cases. Three such cases are depicted in the top panel of Figure 1: in all three cases, the observed mean is $\bar{x} = 1.96$ sigma's away from μ_0 . Under sampling statistics, all three measurements equally reject the null hypothesis, that $\mu = \mu_0$, at the 95% confidence level. And yet common sense clearly tells us that this cannot be the right conclusion in all three cases. Indeed, the Bayes factor, Eq. (18) or (19), correctly recovers the intuitive result (bottom panel of Figure 1): for the curve with $I = 1.0$ (corresponding to non-informative data) model M_0 is mildly disfavored ($B_{01} = 0.5$, or odds of about 2:1 against M_0). For $I = 1.5$ (moderately informative data), evidence starts to accumulate in favor of M_0 ($B_{01} = 1.8$, odds of 9:5 in favor). For strongly informative data, $I = 2.5$, the Bayesian reasoning correctly deduces that the simpler M_0 should be favored ($B_{01} = 18$, odds of 18:1 in favor of M_0). Those conclusions are largely independent of the details of the prior distribution, as shown in Figure 1, where it is apparent that using a Gaussian prior instead of a flat prior does not change significantly the outcome of model comparison, at least for highly informative ($I > 2$) data.

This example illustrates Lindley's paradox (Lindley 1957), in which the Bayesian posterior evidence evaluation favors a model which would be rejected with high confidence by hypothesis testing in a sampling theory approach. While in sampling theory one is only able to disprove models by rejecting hypothesis, in the Bayesian framework evidence can and does accumulate in favor of simpler models, scaling as $I = 1$, see (18) or (19). It is easier to disprove $\mu = \mu_0$, since model rejection is exponential with I , but calculation of the evidence allows to evaluate what the data have to say in favor of an hypothesis, as well. In summary, quoting the number of sigma's away from μ_0 (the parameter) is not always an informative statement to decide whether or not a parameter μ differs from μ_0 . Answering this question is a model comparison issue, which requires the evaluation of the Bayes factor, to which we now turn our attention.

3 APPROXIMATIONS TO THE BAYES FACTOR

In this section we present two approximation methods to compute the Bayes factor. The Laplace approximation relies on the Gaussianity of the pdf, while the Savage-Dickey density ratio is an exact formula which does not make any assumption on the shape of the posterior, and greatly reduces the computational effort needed to calculate the Bayes factor of two nested models. We also present a new technique ("ExPO") to produce a forecast for the Bayes factor probability distribution from a future measurement.

3.1 The Laplace approximation

The evidence for a model M_i is easily calculated by expanding the logarithm of the non-normalized posterior to second order around its peak, which (for a close-to-flat prior) occurs at the best-fit parameter choice θ^* , where the likelihood is maximized. One obtains

$$\ln \frac{P(\mathcal{D}; M_i)}{P(\mathcal{D}; M_0)} = \frac{1}{2} (\theta^* - \theta^*)^T C^{-1} (\theta^* - \theta^*); \quad (22)$$

where C is the covariance matrix of the posterior evaluated at the best-fit point, which can be estimated from the MC samples. This is called Laplace approximation and can be expected to give sensible results if the posterior is reasonably well described by the multidimensional Gaussian of Eq. (22). It is then straightforward to evaluate the evidence by using the approximate form in Eq. (22) for the non-normalized posterior, obtaining

$$Z = P(\mathcal{D}; M_i) = P(\mathcal{D}; M_0) \frac{1}{\sqrt{\det C}}; \quad (23)$$

For flat separable priors of the form in Eq. (4) we can simply write, abbreviating

$$P(\mathcal{D}; M_i) = L(\mathcal{D}; M_i) \frac{1}{\sqrt{\det C}}; \quad (24)$$

an expression which is still approximately correct even if we used non-flat priors, and interpret σ_j as the typical width of the prior pdf (say the standard deviation along the direction of the j th parameter for a Gaussian distributed prior). For a Gaussian prior, it is easy to derive an analytical expression analogous to Eq. (24), but for simplicity we will use the above form.

For the logarithm of the Bayes factor in the Laplace approximation, we then obtain the following handy expression:

$$\ln B_{01} = L_{01} + C_{01} + F_{01}; \quad (25)$$

where we have defined

$$L_{01} = \ln \frac{L(\mathcal{D}; M_0)}{L(\mathcal{D}; M_1)}; \quad (26)$$

$$C_{01} = \frac{1}{2} \ln \left(2 \right)^{d^{(0)} - d^{(1)}} + \ln \frac{\det C^{(0)}}{\det C^{(1)}}; \quad (27)$$

$$F_{01} = \ln \frac{1}{\sqrt{\det C^{(0)}}}; \quad (28)$$

where quantities referring to the model M_i ($i = 0, 1$) are indicated by a superscript (i) . The term L_{01} is the logarithm of the ratio of the best-fit likelihoods. From a frequentist point of view, this quantity is approximately χ^2 distributed, and thus it is common practice to apply to it a goodness-of-fit test to assess whether the extra parameters have produced a "significant" increase of the quality of fit. If M_1 contains more parameters than M_0 , then M_1 should show an improved fit to the data, i.e. we should have $L_{01} < 0$, unless the extra parameters are useless, in which case $L_{01} = 0$. In any case, a goodness-of-fit test alone does not say anything about the structure of the parameter space for the model under consideration, since it is limited to the maximum likelihood point. But Bayesian evidence does contain two further pieces of information, C_{01} and F_{01} , which taken together are sometimes referred to as "Occam's factor". Here we prefer to consider these terms separately to help distinguishing their different origin. The term C_{01} describes the structure of the posterior shape in the Gaussian approximation. Since the determinant is the product of the eigenvalues of the covariance matrix, which represent the standard deviations squared along the corresponding eigenvectors in the parameter space of the model, it follows that if M_0 has a

narrower posterior than M_1 , then $C_{01} < 0$, thereby disfavoring M_0 . This apparent contradiction (how can a model with smaller errors display a smaller evidence?) is resolved when we take into account the term F_{01} , which describes the prior available parameter space under each model. The sum of the terms C_{01} and F_{01} thus disfavors the model with the largest volume of "wasted" parameter space when the data arrive. A more complex model M_1 (having a large number of parameters and thus a large volume of prior accessible parameter space) will naturally fit the data better due to its flexibility, i.e. we will have $L_{01} < 0$, but it will be penalized for introducing extra dimensions in parameter space, i.e. the sum $C_{01} + F_{01}$ will be positive. In sum many, the Bayes factor tends to select the model which exhibits an optimal trade-off between simplicity and quality of fit.

3.2 The Savage-Dickey density ratio

In the case of two nested models, given only a mild assumption on the priors it is possible to derive a simple and exact expression for the evidence. The formula we present below, Eq. (35), goes back to Dickey (1971), who attributed it to Savage, and is therefore called Savage-Dickey density ratio (see also Verdinelli & Wasserman 1995 and references therein).

Consider a model M_1 with two parameters, $(!; \cdot)$ (for simplicity of notation, we take a two parameters case, but the calculations carry over trivially in the multi-dimensional case). Suppose we want compare a submodel M_0 with parameters $(!_0; \cdot)$, with $!_0 = \text{const}$, to the extended model M_1 with an extra free parameter $! \in \mathbb{R}$. In this case, we say that M_0 is nested within M_1 . The Bayes factor B_{01} of Eq. (7) can be evaluated by computing the integrals

$$P(M_0|\mathcal{D}) = \int \pi_0(\cdot) L(\mathcal{D}|\cdot; !_0); \quad (29)$$

$$P(M_1|\mathcal{D}) = \int d!_1(\cdot; !) L(\mathcal{D}|\cdot; !) \quad (30)$$

Here $\pi_0(\cdot)$ denotes the prior over \cdot in model M_0 , and $\pi_1(\cdot; !)$ the prior over $(\cdot; !)$ under model M_1 . Note that, since the models are nested, the likelihood function for M_0 is just a slice at constant $! = !_0$ of the likelihood function in model M_1 , $L(\mathcal{D}|\cdot; !_0)$. We now multiply and divide B_{01} by the number $P(!_0|\mathcal{D}) / P(! = !_0|\mathcal{D}; M_1)$, which is the marginalized posterior for $!$ under M_1 evaluated at $!_0$, and using that $P(!_0|\mathcal{D}) = P(!_0; \mathcal{D}) = P(\cdot; !_0; \mathcal{D})$ at all points, we obtain

$$B_{01} = P(!_0|\mathcal{D}) \int \frac{\pi_0(\cdot) L(\mathcal{D}|\cdot; !_0) P(\cdot; !_0; \mathcal{D})}{\int \pi_1(\cdot; !) P(\cdot; !_0; \mathcal{D})} \quad (31)$$

$$= P(!_0|\mathcal{D}) \int \frac{\pi_0(\cdot) P(\cdot; !_0; \mathcal{D})}{\int \pi_1(\cdot; !) P(\cdot; !_0; \mathcal{D})}; \quad (32)$$

where in the second equality we have used the definition of posterior, namely that $P(!_0; \mathcal{D}) = L(\mathcal{D}|\cdot; !_0) \pi_0(\cdot) = q$. Up to this point we have not made any assumption nor approximation. We now assume that we the prior satisfies

$$\pi_1(\cdot; !_0) = \pi_0(\cdot); \quad (33)$$

which always holds in the (usual in cosmology) case of separable priors, i.e.

$$\pi_1(!; \cdot) = \pi_1(!) \pi_0(\cdot); \quad (34)$$

In other words, by making this assumption we say that the extra parameter of M_1 should not have correlated priors with the parameters of the submodel M_0 . With the assumption (33), Eq. (32) takes the simple form (since $P(\cdot; !_0; \mathcal{D})$ in (32) is the normalized marginal posterior)

$$B_{01} = \frac{P(!_0|\mathcal{D})}{\int \pi_1(\cdot; !_0)} \quad (\text{Savage-Dickey density ratio}). \quad (35)$$

The evaluation of the evidence thus only requires knowing the (properly normalized) value of the marginal posterior at $! = !_0$ under the extended model M_1 . Note that the steps used to arrive at (35) do not involve any assumption about the posterior distribution, and in particular about its normality. While the Laplace approximation can be applied to disconnected models, the Savage-Dickey formula is only valid for nested models.

3.3 Bayes factor forecast: EXP0

A common way to assess the potential of future measurements is the Fisher Matrix analysis (FMA). Given a few parameters of the expected instrument performance, one can readily obtain an estimate of the expected errors on the cosmological parameters of interests (for a detailed account, see e.g. Knox (1995); Kosowsky et al. (1996); Efstathiou & Bond (1999); Rocha et al. (2004)). More precisely, one assumes a fiducial model in parameter space and performs a quadratic expansion of the expected likelihood function around it, equivalent to the Laplace approximation discussed above. Here we explain how to combine this method with the Savage-Dickey density ratio formula to obtain a forecast for the Bayes factor of a future CMB observation. This yields a probability distribution for the expected model comparison results, EXP0 ("Expected Posterior Odds") for short.

For a given compilation of present-day data, consider the elements of a converged MCMC chain in multi-dimensional parameter space. After thinning the chain, we obtain a series of N independent samples from the posterior. The samples are distributed according to the posterior pdf, and their density represents the relative degree of belief in the value of the parameters after we have seen the data. At each sample value $\vec{\theta}_i; i = 1, \dots, N$ we perform a Fisher Matrix analysis assuming $\vec{\theta}_i$ as a fiducial model. This yields for the expected likelihood function a multi-dimensional Gaussian centered at $\vec{\theta}_i$ with covariance matrix $C_i^2 = (F_i^2)^{-1}$, where F_i^2 is the Fisher information matrix (this holds for a given set of fixed instrumental parameters which we do not display explicitly). Writing for the parameters $\vec{\theta} = (!; \cdot)$, where $!$ denotes as before the parameter of interest, the expected pdf for $!$, normalized and marginalized over all other parameters, is simply $N(!_i^2; \vec{\theta}_i)$, where $\vec{\theta}_i = \overline{(\vec{\theta}_i^2)}_{11}$. This holds for separable, at priors along all directions. This assumption is very reasonable, since the likelihood function of future observations will if anything be more peaked than the present one, and we have already remarked that at priors are justified in this case.

From the SD formula, Eq. (35), we then obtain for the expected Bayes factor comparing M_0 : $! = !_0$ against M_1 :

$! \notin !_0$

$$(B_{01})_i^2 = \frac{!_i}{2} \exp \frac{(!_0 - !_i)^2}{2(!_i)^2} \quad (36)$$

where we have dropped the Z functions (see Eq. (17)), since we assume that the likelihood is well within the prior and thus those corrections are negligible. Eq. (36) is the expected Bayes factor assuming that $!_i^?$ is the correct value for $!$, as is implicit in the fact that we have taken $!_i^?$ as a fiducial model for the FMA. We therefore need to weight this result by our present posterior belief that $!_i^?$ is correct, which is given by the pdf $P(!^? | D)$ from current data. Formally, we have

$$P(B_{01} | D) = \int d!^? P(B_{01} | !^?; D) P(!^? | D) \quad (37)$$

$$= \int d!^? \delta(B_{01} - B_{01}^? | !^?) P(!^? | D) \quad (38)$$

where $P(B_{01} | D)$ is the probability of obtaining B_{01} from future data given the present-day data, D , $P(!^? | D)$ is the current posterior for the parameters, δ is the delta function and $B_{01}^? | !^?$ is given in Eq. (36).

The derivation involves the assumption of normality at two levels. The first is implicit in the use of the FMA, while the second requires that the marginalized 1D posterior for $!$ is accurately described by a Gaussian in order for Eq. (36) to be valid. The first assumption is well justified, since the FMA expected errors have proved to give reliable estimates, especially when using "normal parameters" (Kosowsky et al. 2002). As for the second, it is clear that the tails of the posterior are not accurately described by a Gaussian distribution beyond say 3 away from the mean. Thus the numerical value of $(B_{01})_i^?$ from Eq. (36) is not accurate for $|!_0 - !_i^?| \gtrsim 3$. Nevertheless, we can still conclude that such models strongly disfavor M_0 , even though we cannot attach a precise value to the expected odds. This is the reason why we present ExPO results in five bins only (as in Figures 4 and 7), corresponding to the probability of obtaining strong odds in favor of M_1 (odds $> 1 : 100$), moderate odds in favor of M_1 ($> 1 : 10$ but $< 1 : 100$), an undecided result (odds going from $1 : 10$ to $10 : 1$), moderate odds in favor of M_0 ($> 10 : 1$), and strong odds for M_0 ($> 100 : 1$).

Our approach can be extended to the context of Bayesian experiment design, whose goal is to optimize the characteristics of a new observation in order to achieve the maximum science return (often defined in terms of information gain, see Loredo (2003) and references therein for an overview and Bassett (2004); Bassett et al. (2004) for a more cosmology-oriented application). The core of the procedure is the quantification of the utility of an experiment as a function of the experimental design, possibly subject to experimental constraints (such as observing time, sensitivity, noise characteristics, etc). The observing strategy and experiment design are then optimized to maximize the expected utility of the observation. The expected odds distribution is a good candidate for an utility function aimed at model comparison, for it indicates the probability of reaching a clear-cut model distinction thanks to the future observation. The dependence on experimental parameters is implicit in the FMA, and therefore one could imagine optimizing the choice of experimental parameters to maximize the probability of obtaining large posterior odds from the

future data. Since in the present paper we focus on model comparison rather than experiment design, in the following we fix the experimental parameters for the Planck satellite to the value used in Rocha et al. (2004). We leave further exploration of the issue of design optimization and ExPO distribution for future work¹.

4 APPLICATION TO COSMOLOGICAL PARAMETERS

In this section we apply the Bayesian toolbox presented above to three cosmological parameters which are central for our understanding of the concordance model: the spectral index of scalar (adiabatic) perturbations, the spatial curvature of the Universe and an isocurvature CDM component to the initial conditions for cosmological perturbations.

4.1 Parameter space and cosmological data

We include in our analysis the first-year WMAP data (Bennett et al. 2003; Hinshaw et al. 2003) (temperature and polarization) with the routine for computing the likelihood supplied by Verde et al. (2003), as well as the CBI (Readhead et al. 2004), VSA (Dickinson et al. 2004) and ACBAR (Goldstein et al. 2003) measurements of the CMB. All of these data-sets combined together are denoted by the label "WMAPext". In addition to the CMB data, we also include constraints on the real-space power spectrum of galaxies from the Sloan Galaxy Redshift Survey (SDSS) (Tegmark et al. 2004a). To be conservative, we restrict ourselves to a range of scales over which the fluctuations are assumed to be in the linear regime ($k < 0.1 h^{-1} \text{Mpc}$), which leaves us with $N = 14$ data points. We shall also take into account the HST measurement (Freedman et al. 2001) of the Hubble parameter in form of a Gaussian datum with mean $h = 0.72$ and spread $= 0.08$, where we denote by $h = H_0 = 100 \text{ km sec}^{-1} \text{Mpc}^{-1}$ the present value of the dimensionless Hubble parameter. Furthermore, we shall also consider the latest supernovae observations data (Riess et al. 2004).

We make use of the publicly available codes² CAMB and CosmoMC Lewis & Bridle (2002) to compute the CMB and matter power spectra and to construct Monte Carlo Markov Chains (MCMC) in parameter space. The Monte Carlo (MC) is performed using "normal parameters" (Kosowsky et al. 2002), in order to minimize non-Gaussianity in the posterior pdf. In particular, we sample uniformly over the physical baryon and cold dark matter (CDM) densities, $!_b = b h^2$ and $!_c = c h^2$, expressed in units of $1.88 \times 10^{-29} \text{ g cm}^{-3}$; the ratio of the angular diameter distance to the sound horizon at decoupling, r_s , the optical depth to reionization τ (assuming sudden reionization and imposing an upper prior $\tau < 0.3$) and the logarithm of the adiabatic amplitude for the primordial fluctuations, $\ln 10^{10} A_s$. Using normal parameters for the CMB analysis is

¹ An add-on ExPO module for the CosmoMC package is publicly available from the web page: <http://theory.physics.unige.ch/~trotta/html/software.htm>

² Available from the website: <http://cosmologist.info/>.

especially important to improve the accuracy of the Laplace approximation. We always take flat priors unless otherwise stated. When combining the matter power spectrum with CMB data, we marginalize analytically over a bias b considered as an additional nuisance parameter. Throughout we assume three massless neutrino families and no massive neutrinos (for constraints on these quantities, see instead e.g. Bowen et al. 2002; Trotta et al. 2003; Pierpaoli 2003; Hannestad 2003), we fix the primordial Helium mass fraction to the value predicted by Big Bang Nucleosynthesis (see e.g. Trotta & Hansen 2004) and we neglect the contribution of gravitational waves to the CMB power spectrum.

4.2 The scalar spectral index

As a first application of the approximations outlined above to the problem of model selection from current cosmological data, we consider the scalar spectral index for adiabatic perturbations, n_s . We compare the evidence in favor of a scale invariant index ($H_0 : n_s = 1$), also called an Harrison-Zel'dovich (HZ) index, with a more general model of single-field inflation, in which we do not require the spectral index to be scale invariant ($H_1 : n_s \neq 1$). In this example, our M_1 , which we will call for brevity generic inflation, contains one extra parameter than the HZ model, namely n_s . The Bayes factor for these two models is computed in the following.

Within the framework of slow-roll inflation, the prior allowed range for the spectral index can be estimated by considering that $n_s = 1 - 6 + 2$, where and are the slow-roll parameters. If we assume that is negligible, then $n_s = 1 + 2$. If the slow-roll conditions are to be fulfilled, ≤ 1 , then we must have ≤ 0.1 , which gives $0.8 \leq n_s \leq 1.2$. Hence a ballpark estimate of the prior range is $n_s = 0.4$. Let us first make use of the Laplace approximation, Eq. (25), which assumes that the posterior pdf is close to Gaussian, which indeed is by eye quite accurately the case, at least for the bulk of the pdf (see Figure 2). The HZ model is nested within the generic inflation model, and therefore all the prior ranges for the common parameters cancel out from the F_{01} term in Eq. (25), and we do not need to specify them at all. Thus using a flat prior on the extra parameter n_s of width $n_s = 0.4$, as argued above, we have $F_{01} = \ln(n_s) = -0.9$. The ratio of the best likelihoods depends on the data used, going from $L_{01} = 1:1$ for CMB alone, to $L_{01} = 2:3$ including SDSS information (further adding the HST measurement does not change the result significantly), indicating that adding n_s as an extra parameter improves the quality of L . The posterior structure is given by the covariance matrices estimated from the MC samples: for CMB alone, we have $C_{01} = 2.6$, rising to $C_{01} = 3.0$ including SDSS. Summing together all the contributions to the evidence, we find $\ln B_{01} = 0.6$, which corresponds to posterior odds of about 2 : 1 in favor of the HZ case for CMB alone, which drop to 4 : 5 ($\ln B_{01} = 0.2$) when adding SDSS. The evidence of present-day data is thus essentially non-informative regarding the question of the scale invariance of n_s , and this despite the fact that the combined data have $I = 2.0$, which is to say that the mean of the posterior is 2 away from $n_s = 1$ (see Table 1).

We now determine the Bayes factor using the Savage-Dickey density ratio instead, which is valid since the HZ model is nested within the generic inflation model and the

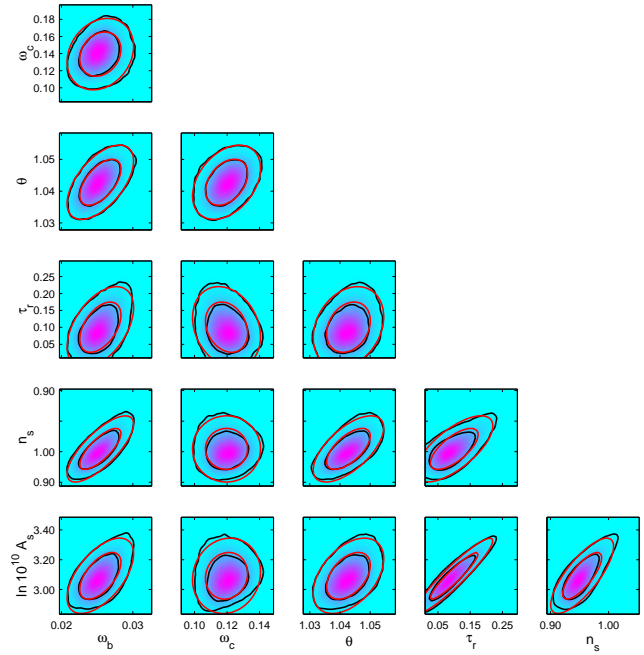


Figure 2. Laplace approximation to the 6-dimensional posterior, including n_s as free parameter and using WMAP ext + SDSS data. For all couples of parameters, panels show contours enclosing 68% and 95% of joint probability from 210MC samples (black contours), along with the Laplace approximation (red ellipses). It is clear that the Laplace approximation captures the bulk of the posterior volume in parameter space in this case where there is little non-Gaussianity in the posterior pdf.

assumption of separable priors needed to derive (35) is also fulfilled. The evidence in favor of the HZ model, B_{01} , can then be evaluated from (35), provided we correctly normalize the 1D marginalized posterior $P(n_s | D)$. The normalization constant can easily be found by numerically integrating the non-normalized 1D posterior. Since this is a 1D integral, a simple trapezoidal rule is accurate enough for our goal. The normalized 1D posteriors for two different compilations of data-sets are plotted in Figure 3. The prior range is as before $n_s = 0.4$, but in this case we choose a Gaussian prior (instead of a flat prior) centered on $n_s = 1$ and with standard deviation $n_s = 2$, which gives $\ln(n_s = 1) = 2.0$ in Eq. (35) (choosing a flat prior instead would have given $\ln(n_s = 1) = 2.5$, thus reducing the odds by 20%). For the evidence from CMB data alone we obtain again odds of 2 : 1 ($\ln B_{01} = 0.7$) in favor of the HZ model, but when SDSS information is added (with or without the HST measurement) this reduces to about equal odds for the two models. When including SDSS, I increases by about 25%, but we still have only $I = 1.0$. As argued in section 5.1, a robust evidence determination would require I to be of order 2 at least. The Savage-Dickey criterium and the Laplace approximation are in good agreement, see Table 1. We have explicitly checked that the tails of the distribution are not important for the numerical accuracy of this result by running the MC chains at higher temperature, then cooling them. We have also changed the number of bins in which the chains' points are divided. In all cases, the evidence is scarcely affected.

From the current posterior pdf we can produce an

Table 1. Summary of model comparison results for the H_Z , scale invariant ($n_s = 1$) model against the generic inflation ($n_s \neq 1$) case, using a slow-roll inflation motivated prior. Present-day data are essentially non-informative regarding the question of whether n_s is scale invariant or not. The Laplace and Savage-Dickey (SD) methods yield similar results.

Data	HZ vs. $n_s \neq 1$			
	I	$\ln B_{01}$ (SD)	$\ln B_{01}$ (Laplace)	Odds
WMAPext	1.3	0.8	0.7	0.6
WMAPext+SDSS	2.0	1.0	0.0	-0.2

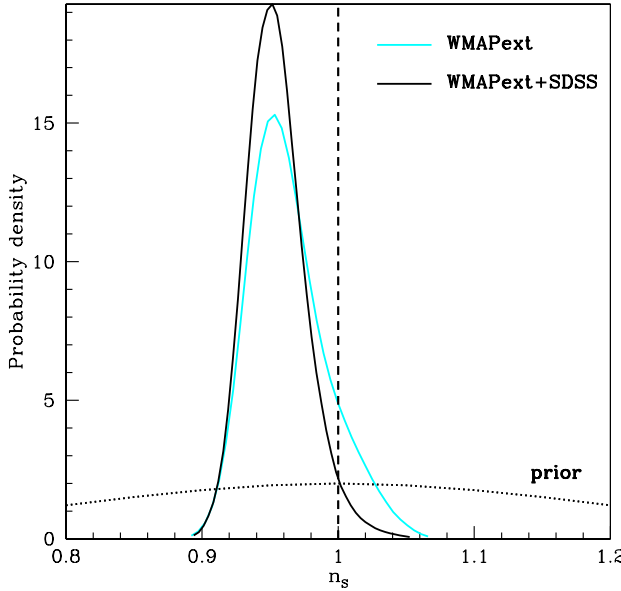


Figure 3. Evaluation of the Bayes factor comparing a model without spectral tilt ($n_s = 1$, vertical dashed line) against a model with $n_s \neq 1$, using the SD density ratio. We plot the 1D marginalized posterior pdf's for n_s from the MC samples, properly normalized to unity probability content, along with the Gaussian prior adopted (black dotted line). The Bayes factor can be read off as the ratio of the posterior to the prior at the point $n_s = 1$. The bins have been smoothed with a Gaussian window for display purposes only.

ExPO forecast for the Planck satellite³ (an European Space Agency CMB mission scheduled for launch in 2007) following the procedure outlined in Section 3.3. The result is shown in Figure 4, where we plot the probability of model comparison results (comparing $n_s = 1$ against $n_s \neq 1$), conditional on the current posterior from WMAPext+SDSS. Using E-polarization alone, the bulk of the probability lies in the non-informative region, where the expected odds are of order 1 : 1. This means that with E-polarization measurements only, Planck will most probably not be able to give a high-odds answer to the question of whether we need a spectral tilt or not. But when temperature information is taken into account, 90% of the probability lies in the high-odds region where $n_s = 1$ is disfavored by more than 1 : 100. This is the main result of our forecast, and a consequence of the fact that the most probable models under current data

are clustered around $n_s = 0.95$ (see Figure 2). Given the expected reduction of the posterior width for n_s for Planck (as predicted by the FMA), such models disfavor $n_s = 1$ with high-odds and correspond to the peak in the ExPO. It is interesting to notice that the large leverage of multipole numbers provided by the accurate mapping of the temperature spectrum will be fundamental for this high-odds model comparison result. We emphasize once more that the ExPO are conditional to the current posterior, which means that the forecast is reliable provided there will be no major systematical shift in the parameter determination with respect to present-day data. In other words, the ExPO only take into account the statistical properties of our knowledge, a point hardly worth highlighting (if we knew the outcome of a future measurement, it would be pointless to carry it out). On the other hand, the ExPO procedure goes a step further that the FMA, in that it does not assume a fiducial model for its forecast, but it does consider the current uncertainty in the parameter value.

In summary, current cosmological data do not allow to draw highly-informative conclusions about the need for a spectral tilt of scalar perturbations, in agreement with the findings of (Beltran et al. 2005) obtained using thermodynamical integration. However, we also found that there is about 90% probability that future Planck measurements will provide clear-cut evidence against a scale invariant index. This result is in disagreement with the conclusion obtained by Liddle (2004) based on the information criteria, i.e. that $n_s \neq 1$ should be rejected as an useful parameter. It seems to us that the information criteria alone do not take into account either the structure of the posterior volume in parameter space, or salient features of the models under scrutiny, i.e. the prior allowed parameter range. As our examples show, a proper evaluation of the Bayes factor yields much more useful information.

4.3 The spatial curvature

The case of spatial curvature is more subtle, since the posterior pdf for h strongly depends on the data one decides to consider. In particular, leaving the Hubble parameter h completely free in the range 0.16 to 1.0 and allowing for spatial curvature at the same time results in the well-known "geometrical degeneracy" when using CMB information only (see e.g. Easther & Bond (1999); Melchiorri & Gorini (2001)). This degeneracy, which is almost exact for the CMB, can be only partially broken by adding matter power spectrum measurements. Only additional information on the value of h and/or inclusion of supernovae data can constrain significantly (Tegmark et al. 2004b). Those facts are well

³ See the website: <http://astro.estec.esa.nl/Planck>.

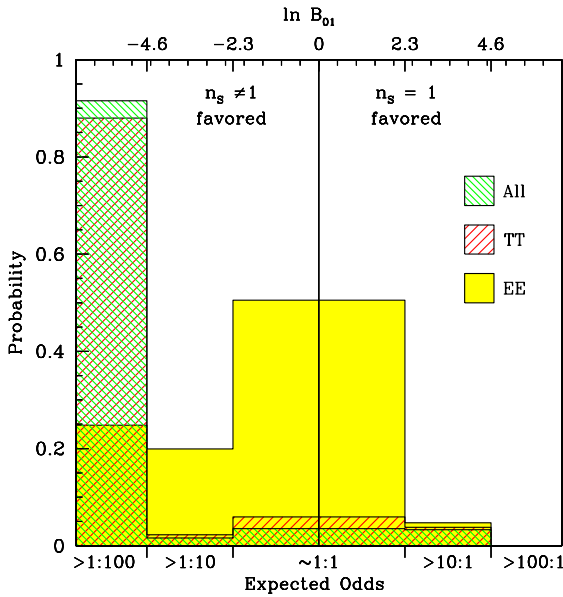


Figure 4. ExPO for the Planck satellite nominal mission, comparing a model with ($n_s \neq 1$) and without ($n_s = 1$) a spectral tilt. While the E-polarization spectrum measurement alone (EE) will be rather non-informative, there is about 90% probability that temperature (TT), E-polarization and TE-correlation measurements together (All) will strongly disfavor $n_s = 1$ (with odds larger than 1 : 100). The accurate mapping of the high- $\ln B_{01}$ region of the temperature spectrum (TT) is essential for achieving this result. The forecast is conditional on the current posterior from WMAP+SDSS for the cosmological parameters, see the explanations in section 3.3. This ExPO distribution is based on about 5000 samples (after thinning).

known, and we now discuss the consequences in terms of the evidence for a flat Universe.

We proceed analogously as in the previous section, and evaluate the Bayes factor for $\Omega_k = 0$ (flat Universe) against a model with $\Omega_k \neq 0$. As discussed above, we only need to specify the prior distribution for the parameter of interest, namely Ω_k . We choose a flat prior of width $\Delta\Omega_k = 2.0$ centered around $\Omega_k = 0$, for we know that the universe is not empty (thus $\Omega_k < 1.0$, setting aside the case of $\Omega_k < 0$) nor largely overclosed (therefore $\Omega_k > 1$ is a reasonable range, see 5.3 for further comments). In agreement with previous works, we obtain that the marginalized posterior pdf for Ω_k tends to peak at values $\Omega_k < 0$, regardless of the data one uses (see Figure 5). In order to answer the question of whether this is significant enough as to justify the conclusion that the Universe is closed, we apply the SD criterium and the Laplace approximation to various combination of data. Our findings are summarized in Table 2.

The CMB alone is unable to significantly constrain because of the fundamental geometrical degeneracy, and thus we do not consider this case. Even CMB and SDSS data together allow for a wide range of negative values for the curvature. This results in about equal odds for a flat or a curved model using the SD ratio, which gives $\ln B_{01} = 0.4$. Adding SN Ia observations drastically reduces the range of the posterior, since their degeneracy direction is almost orthogonal to the geometrical degeneracy. The pdf still peaks

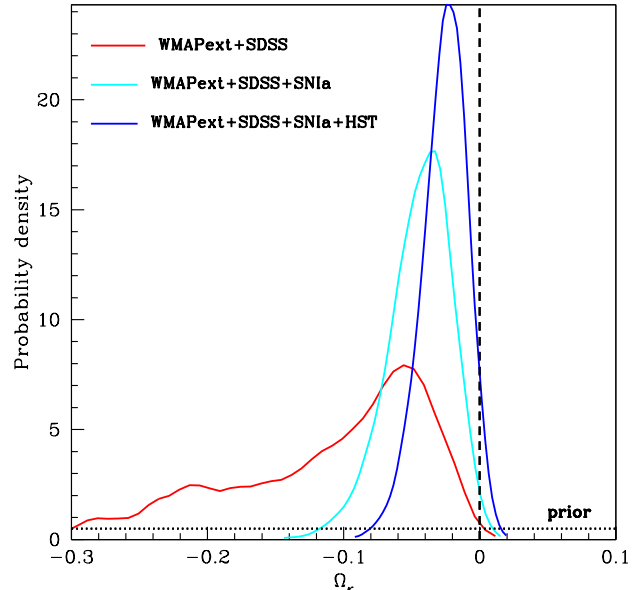


Figure 5. Normalized posterior probabilities for $\Omega_k \neq 0$ from different combinations of data-sets. Measurements of the CMB and of the matter power spectrum (curve WMAPext + SDSS) are not informative on the curvature because of the geometrical degeneracy. Adding external information on the Hubble parameter or on an orthogonal combination of the matter and cosmological constant content allows to obtain moderate evidence in favor of a flat Universe, with odds of about 14 : 1 (narrowest curve).

at 1 : 3 from $\Omega_k = 0$, but now the value of the posterior at $\Omega_k = 0$ is larger, thus favoring a flat Universe with odds of about 3 : 1. Adding the HST measurement for the Hubble parameter makes a real difference, since the handle on the value of Ω_k breaks the geometrical degeneracy. When all of the data is taken into account, we obtain a Bayes factor which favors the flat model with odds of about 14 : 1. In Table 2 we give a range of values for $\ln B_{01}$ which reflects the results obtained using different binning schemes and performing the MC at different temperatures for each combination of data. We emphasize that this is not a statistical uncertainty, only the typical spread observed in different runs, which gives an indication of the level of numerical accuracy of the result. In contrast to the case of the scalar spectral index, it appears that the case of curvature is more sensitive to numerical issues of the MC run. However, an order of magnitude evaluation of the posterior odds is enough for our purpose, so a numerical error well below unity in $\ln B_{01}$ is perfectly acceptable in this context.

The agreement with the Laplace approximation is less precise in this case, since allowing for curvature introduces non-Gaussian features in the posterior distribution which spoil the accuracy of the Laplace approximation (see Figure 6), especially for the less informative cases. Nevertheless, we still correctly recover the trend of the evidence, which accumulates in favor of the flat model as more information is added, see Table 2. As more data-sets are included, the information content I increases, signalling that we are entering the region of high-significance for the evidence. In fact, the combined data-sets (WMAPext+SDSS+HST+SN Ia)

Table 2. Summary of model comparison between a flat Universe ($\kappa = 0$) and a curved one ($\kappa \neq 0$), assuming a prior $\kappa = 2.0$, stemming from the fact that the Universe is not empty nor clearly overclosed. The quantity I and the information content I are defined in Eqs. (9) and (21), respectively. Combination of all data yields a moderate evidence for a flat Universe. The odds in the last column refer to the SD ratio result.

Data	Flat vs. curved Universe			
	I	$\ln B_{01}$ (SD)	$\ln B_{01}$ (Laplace)	Odds
WMAP ext+ SD SS	1.4	1.4	0.4	0.5
WMAP ext+ SD SS+ SN Ia	1.3	1.8	1.0 :: 1.2	0.4 :: 0.6
WMAP ext+ SD SS+ HST + SN Ia	1.0	2.0	2.5 :: 2.7	2.3 :: 2.6

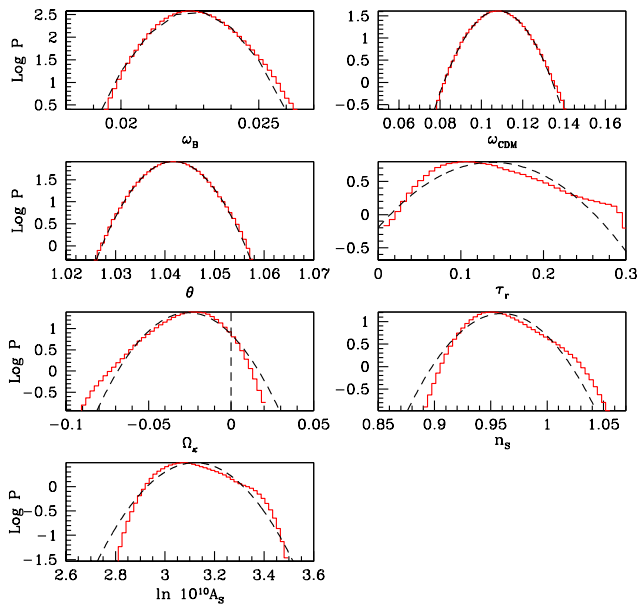


Figure 6. The Laplace approximation (dashed, black parabolae) compared with the 1D marginalized posterior from the MC samples (red histograms), using the most informative combination of present-day data. Discrepancies are visible especially in the tails of τ_r , n_s and A_s .

are much more informative than CMB and SD SS only ($I = 2.0$ against $I = 1.4$). It is clear from this example that evidence and information content together provide a more complete description of the power of data than I alone (see below 5.1).

The ExPO for Planck (Figure 7) indicate that even in the future CMB alone will not be able to distinguish between the two models, since most of the probability is concentrated in the non-informative region, regardless of the CMB information used. This result is expected on the grounds of the fundamental geometrical degeneracy which affects CMB measurements, which cannot be broken even with cosmological variance limited observations. As a consequence, it will be imperative to improve on complementary observations which do break the geometrical degeneracy in order to obtain higher-odds result. In summary, most of the evidence in favor of a flat Universe comes from the Hubble parameter determination, a key result which will still hold true for future, high-quality CMB observations.

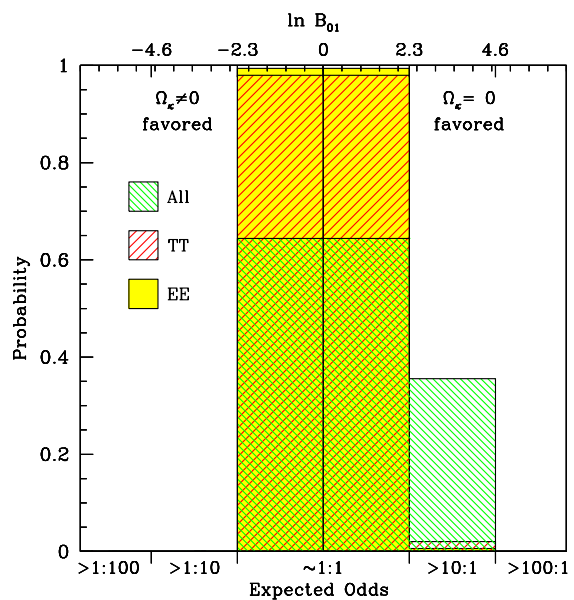


Figure 7. ExPO for the Planck satellite, comparing the odds in favor of a curved ($\kappa \neq 0$) against a flat Universe. The forecast is conditional on the current most informative data, namely WMAP ext+ SD SS+ SN Ia+ HST, but it takes into account Planck data only. Therefore, the geometrical degeneracy prevents Planck from achieving highly informative odds. With CMB information only, it will not be possible to confirm or disprove $\kappa = 0$ with high evidence. This calls for improvements in independent measurements that break this degeneracy, e.g. Hubble parameter determination.

4.4 The CDM isocurvature contribution

The third case we consider is the possibility of a cold dark matter (CDM) isocurvature contribution to the primordial perturbations. For a review of the possible isocurvature modes and their observational signatures, see e.g. Trotta (2004). Determining the type of initial conditions is a central question for our understanding of the generation of perturbations, and has far reaching consequences for the model building of the physical mechanism which produced them. Constraints on the isocurvature fraction have been derived in several works, which considered different phenomenological mixtures of adiabatic and isocurvature initial conditions (Pierpaoli et al. 1999; Amendola et al. 2002; Trotta et al. 2001, 2003; Trotta & Durrer 2004; Bucher et al. 2004; Trotta et al. 2003; Valivita & Muñoz 2003; Beltran et al. 2004; Moodley et al. 2004; Kurki-Suonio et al. 2004). While current data require that the initial conditions are preva-

lently adiabatic in nature, a subdominant contribution of isocurvature modes cannot be excluded using parameter estimation techniques. Recently, the question of isocurvature modes has been tackled by Beltran et al. (2005) using a Bayesian evidence approach similar in spirit to the one presented here. Our treatment has the advantage of being much more economical in terms of the requested computing power, since it avoids the costly thermodynamical integration used in Beltran et al. (2005).

Since the goal of this work is not to present a detailed analysis of isocurvature contributions, but rather to give a few illustrative applications of Bayesian model selection, we restrict our attention to the comparison of a purely adiabatic model against a model containing a CDM isocurvature mode totally correlated or anti-correlated. For simplicity, we also take the isocurvature and adiabatic mode to share the same spectral index, n_s . This phenomenological set-up is close to what one expects in some realizations of the curvaton scenario, see e.g. Gordon & Lewis (2003); Lyth & Wands (2003); Lazarides et al. (2004).

We compare model M_0 , with adiabatic fluctuations only, with M_1 , which has a totally (anti)correlated isocurvature fraction

$$f_{\text{iso}} = \frac{S}{\Omega}; \quad (39)$$

where Ω is the primordial curvature perturbation and S the entropy perturbation in the CDM component (see Trotta (2004); Lazarides et al. (2004) for precise definitions). The sign of the parameter f_{iso} defines the type of correlation. The definition of positive or negative correlation being a matter of convention, we adopt the same notation as in Lazarides et al. (2004), so that a positive (negative) correlation, $f_{\text{iso}} > 0$ ($f_{\text{iso}} < 0$), corresponds to a negative (positive) value of the adiabatic-isocurvature CMB correlator power spectrum on large scales. We choose f_{iso} as the relevant parameter for model comparison because of its immediate physical interpretation as an entropy-to-curvature ratio, but this is only one among several possibilities.

In the absence of a specific model for the generation of the isocurvature component, there is no stringent physical motivation for setting the prior on f_{iso} . A generic argument is given by the requirement that linear perturbation theory be valid, i.e. $|\Omega| \ll 1$. This however does not translate into a prior on f_{iso} , unless we specify a lower bound for the curvature perturbation. In general, f_{iso} is essentially a free parameter, unless the theory has some built-in mechanism which sets a (small) scale for the entropy amplitude. This however requires digging into the details of specific realizations for the generation of the isocurvature component. For instance, the curvaton scenario predicts a large f_{iso} if the CDM is produced by curvaton decay and the curvaton does not dominate the energy density, in which case $|f_{\text{iso}}| \approx r^{-1} \ll 1$, since the curvaton energy density at decay compared with the total energy density is small, $r_{\text{curv}} = r_{\text{tot}}^{-1} \ll 1$ (Lyth & Wands 2003; Gordon & Lewis 2003). Once the details of the curvaton decay are formulated, it might be possible to argue for a theoretical lower bound on r , which gives the prior range for the predicted values of f_{iso} .

In the absence of a compelling theoretical motivation for setting the prior, we can still appeal to another piece

of information which is available to us before we actually see any data: the expected sensitivity of the instrument. In fact, we can assess the possible outcomes of a measurement by investigating the sensitivity of the experiment (given its forecasted noise levels) in parameter space. This allows us to limit the a priori accessible parameter space for a specific observation on the grounds that it is pointless to admit values which the experiment will not be able to measure. For the case of f_{iso} , there is a lower limit to the a priori accessible range dictated by the fact that a small isocurvature contribution is masked by the dominant adiabatic part. Conversely, the upper range for f_{iso} is reached when the adiabatic part is hidden in the prevailing isocurvature mode. In order to quantify those two bounds, one runs a Fisher matrix forecast assuming noise levels appropriate for the measurement under consideration, thus determining which regions of parameter space can be explored by the observation. Such a prior is therefore motivated by the expected sensitivity of the instrument, rather than by theory. The prior range for a scale-free parameter thereby becomes a computable quantity which depends on our prior knowledge of the experimental apparatus.

We have performed a FM forecast in the (Ω, β) plane, whose results are plotted in Figure 8 for the WMAP expected sensitivity. We use a grid equally spaced in the logarithm of the adiabatic and isocurvature amplitudes, in the range $10^{-6} \leq \Omega \leq 10^{-5}$ and $10^{-8} \leq \beta \leq 10^{-2}$. For each pair (Ω, β) the FM yields the expected error on the amplitudes as well as on f_{iso} . The expected error however also depends on the fiducial values assumed for the remaining cosmological parameters. In order to take this into account, at each point in the (Ω, β) grid we run 40 FM forecasts changing the type of correlation ($\text{sign}(S) = \pm 1$), the spectral index ($n_s = 0.8 \pm 0.1$ with a step of 0.1) and the optical depth to reionization ($r = 0.05 \pm 0.35$ with a step of 0.1). The other parameters $(\Omega, \beta, \Omega_b, \Omega_c)$ are fixed to the concordance model values, since Ω, β are mostly correlated with $\Omega, \Omega_b, \Omega_c$ and thus only the fiducial values assumed for the latter two parameters have a strong impact on the predicted errors of the amplitudes. We then select the best and worst outcome for the expected error on f_{iso} , in order to bracket the expected result of the measurement independently on the fiducial value for r, n_s . Notice that at no point we make use of real data. By requiring that the expected error on f_{iso} be of order 10% or better, we obtain the a priori accessible area in amplitude space for WMAP, which is shown in Figure 8.

It is apparent that f_{iso} cannot be measured by WMAP if either Ω or β are below about 10^{-5} , in which case the signal is lost in the detector noise. For amplitudes larger than 10^{-5} , $|f_{\text{iso}}| = 1$ is accessible to WMAP with high signal-to-noise independently on the value of r, n_s , while $|f_{\text{iso}}| = 0.4$ can be measured only in a few cases for the most optimistic choice of parameters. As an aside, we notice that if we restrict our attention to models which roughly comply with the COBE measurement of the large scale CMB power (blue/solid lines in Figure 8), then WMAP can only explore the subspace of anti-correlated isocurvature contribution (right of the cusp) and only if $r > 7 \times 10^{-5}$. On the other end of the range, we can see that $|f_{\text{iso}}| = 100$ is about the largest value accessible to WMAP, at least for $\Omega > 5 \times 10^{-6}, \beta > 10^{-2}$. There is a simple physical reason for the asymmetry of the accessible range

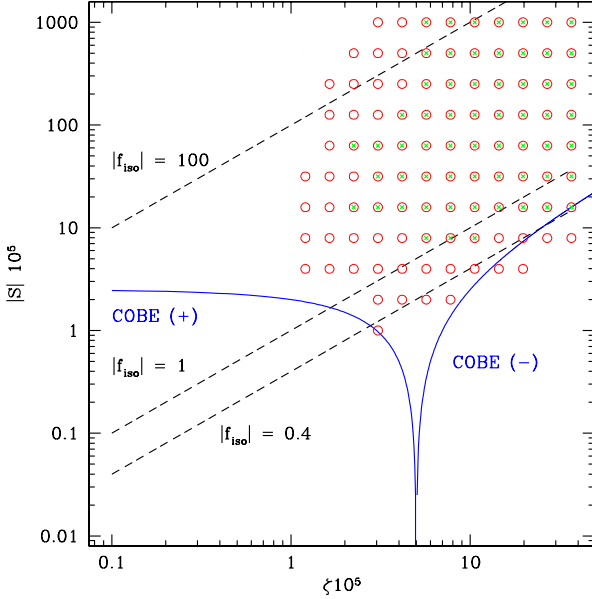


Figure 8. Sensitivity analysis for WMAP. The a priori accessible parameter space in the $(S; \xi)$ plane is obtained by requiring better than 10% accuracy on $|f_{\text{iso}}|$ in the Fisher matrix error forecast (open circles for the best case, crosses for the worst case, depending on the fiducial values of r, n_s and on the sign of the correlation). This translates into a prior accessible range $0.4 < |f_{\text{iso}}| < 100$ (diagonal, dashed lines), but only if $|\xi| > 10^5$. Models which roughly satisfy the COBE measurement of the large scale CMB anisotropies ($T = T_0 = 10^5$) lie on the blue/solid line and have positive (negative) correlation left (right) of the cusp.

around $|f_{\text{iso}}| = 1$: a small isocurvature contribution can be overshadowed by the adiabatic mode on large scales due to cosmic variance, but a subdominant adiabatic mode is still detectable even in the presence of a much larger isocurvature part, because the first adiabatic peak at ~ 200 sticks out from the rapidly decreasing isocurvature power at that scale (at least if the spectral tilt is not very large, as in our case). In conclusion, the values of $|f_{\text{iso}}|$ which WMAP can potentially measure with high signal-to-noise are approximately bracketed by the range $0.4 \leq |f_{\text{iso}}| \leq 100$, assuming that $\xi > 10^5$. Given the fact that most of the prior volume lies above $|f_{\text{iso}}| = 1$, we can take a flat prior on f_{iso} centered around $f_{\text{iso}} = 0$, with a range $-100 \leq f_{\text{iso}} \leq 100$, or $f_{\text{iso}} = 200$. As we shall see below, it is this large range of a priori possible values compared with the small posterior volume which heavily penalizes an isocurvature contribution due to the Occam's razor behavior of the Bayes factor.

The marginalized posterior on f_{iso} for different combinations of data is plotted in Figure 9, which shows that current data yield only upper bounds on the CDM isocurvature fraction, in agreement with previous works. The posterior for CMB alone is slightly skewed towards negative correlation, while inclusion of large scale structure data shifts the peak to positive correlation. For CMB alone, the spread of the posterior is of order 0.1, which lies an order of magnitude below the level ($|f_{\text{iso}}| = 1$) at which an isocurvature signal would have stood out clearly from the WMAP noise. The

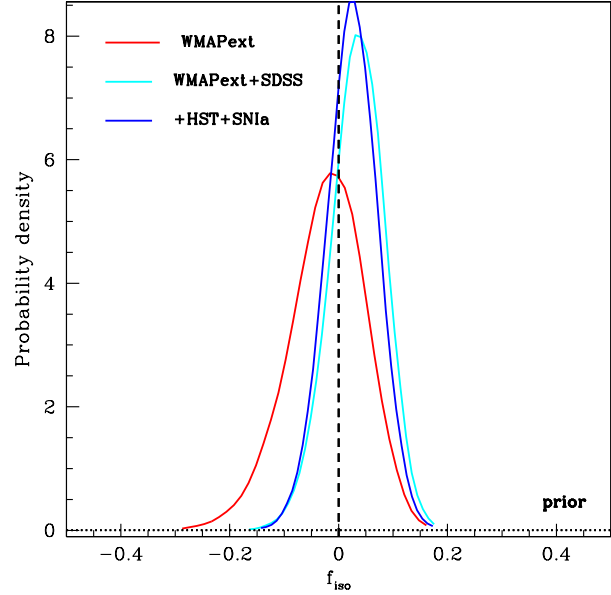


Figure 9. Normalized 1D marginalized posterior pdf for the entropy-to-curvature ratio f_{iso} for a totally (anti)correlated isocurvature CDM component.

Bayes factors from the SD formula and the Laplace approximations are displayed in Table 3. Strong odds in favor of the purely adiabatic model (of order 1000 : 1 or larger) are primarily the consequence of the large volume of "wasted" parameter space for the isocurvature contribution, and a fine example of automatic Occam's razor built into the Bayes factor. A model which allows for a range of possible values for f_{iso} which turns out to be much larger than the posterior bound is disfavored because unnecessarily complex. In other words, the introduction of a new scale-free isocurvature amplitude is generically unwarranted by data, a feature already remarked by Lazarides et al. (2004).

This result differs from the findings of Beltran et al. (2005), who considered an isocurvature CDM admixture to the adiabatic mode with arbitrary correlation and spectral tilt and concluded that there is no strong evidence against mixed models (odds of about 3 : 1 in favor of the purely adiabatic model). While their setup is not identical to the one presented here and thus a direct comparison is difficult, we believe that the key reason of the discrepancy can be traced back to the different basis for the initial conditions parameter space. Instead of the isocurvature fraction f_{iso} , Beltran et al. employ the parameter β describing the fractional isocurvature power, which is related to f_{iso} by

$$= \frac{f_{\text{iso}}^2}{1 + f_{\text{iso}}^2} : \quad (40)$$

The infinite range $0 \leq |f_{\text{iso}}| < 1$ corresponds in this parameterization to a compact interval $[0:1]$ for β (or $[1:1]$ for β'), over which they take a flat prior for the variable β (or β'). Flat priors over β or β' correspond to the priors over $|f_{\text{iso}}|$ depicted in Figure 10, which cut away the region of parameter space where $|f_{\text{iso}}| > 1$. As a consequence, the Occam's razor effect is suppressed and the resulting odds in favor of the purely adiabatic model are much smaller than

Table 3. Summary of model comparison results for a purely adiabatic model versus a model with mixed adiabatic-CDM isocurvature initial conditions, with a prior on f_{iso} appropriate for WMAP noise levels. The CDM isocurvature mode has the same spectral index as the adiabatic mode, and is either totally correlated or anti-correlated. The Savage-Dickey and the Laplace approximations are in good agreement, and strongly favor purely adiabatic perturbations, as a consequence of Occam's razor.

Data	Purely adiabatic vs mixed adiabatic-CDM isocurvature			
	I	$\ln B_{01}$ (SD)	$\ln B_{01}$ (Laplace)	Odds
WMAP ext	0.3	3.1	7.2	1300 : 1
WMAP ext+SDSS	0.8	3.3	7.3	1500 : 1
WMAP ext+SDSS+HST+SN Ia	0.5	3.3	7.5	1800 : 1

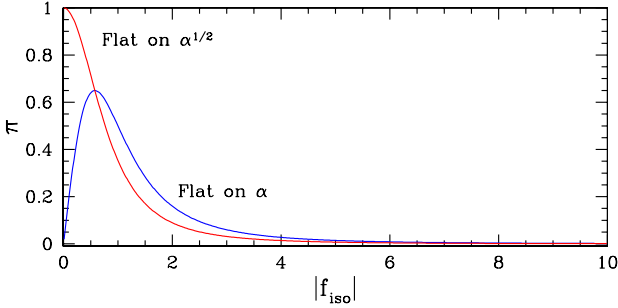


Figure 10. Equivalent priors on $|f_{\text{iso}}|$ corresponding to the priors used in Beltran et al. (2005) for the parameters α and β . Both priors cut away the parameter space $|f_{\text{iso}}| > 1$, thus reducing the Occam's razor effect caused by a scale-free parameter. The odds in favor of the purely adiabatic model thus become correspondingly smaller. Model comparison results can depend crucially on the variables adopted.

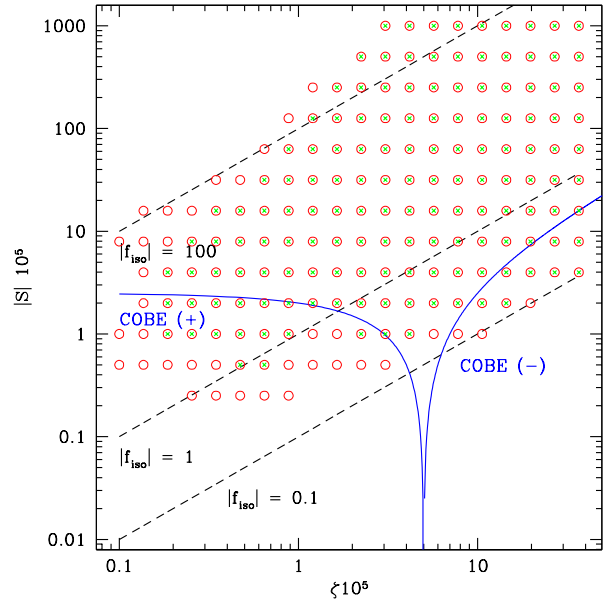


Figure 11. Sensitivity analysis for Planck, with symbols as in Figure 8. Planck will explore the range $0.1 < |f_{\text{iso}}| < 100$ (diagonal, dashed lines) with high signal-to-noise, for $(\alpha; \beta)$ as low as 10^{-4} . Positively correlated models compatible with the COBE measurement of large scale CMB power will be within Planck's potential (blue/solid line left of the cusp), a parameter region which cannot be reached by WMAP (compare Figure 8).

in our case. This example illustrates that model comparison results can depend crucially on the underlying parameter space. We comment further on this point in Section 5.3.

Finally, given the already rather large odds in favor of a purely adiabatic model coming from present-day data, it is pointless to carry out a full EXPO analysis for Planck. The prior accessible range over $|f_{\text{iso}}|$ for Planck can be assessed using the noise levels for the satellite, obtaining the expected sensitivity plot of Figure 11. The parameter space which Planck will be able to explore with high signal-to-noise is roughly bracketed by $0.1 < |f_{\text{iso}}| < 100$, with the accessible region extending to amplitudes as low as 10^{-4} , an order of magnitude below the capability of WMAP. As an interesting side result, we notice that Planck will explore with high sensitivity the space of positively correlated models compatible with the large-scale power measured by COBE (left branch of the solid, blue line in Figure 11), a region where WMAP does not have the potential for measuring f_{iso} . Furthermore, if the isocurvature fraction is just below current sensitivity levels, Planck will be able to obtain a high signal-to-noise measurement. In the absence of the latter, the upper limit on $|f_{\text{iso}}|$ will be of order 0.01 . Taking again a flat prior of range $|f_{\text{iso}}| = 200$ around $f_{\text{iso}} = 0$, as motivated by Figure 11, we conclude that the posterior odds in favor of the purely adiabatic model will increase to about $10^4 : 1$.

5 DISCUSSION

5.1 Information is the key

We have already pointed out that the Bayes factor is really a function of two parameters, α and the information content I. If the marginalized posterior for the parameter of interest β is well described by $N(\hat{\beta}; \hat{\sigma}_\beta)$ and we assume separable priors, then the Savage-Dickey formula, Eq. (35), reduces to Eq. (18) for a flat prior of range β or Eq. (19) if we use $N(\beta_0; \sigma_\beta^2)$ as prior. For this last case, we plot in Figure 12 contours of $\log_{10} B_{01} = \text{const}$ for $\text{const} = 1; 2$ in the $(\alpha; I)$ plane. Such contours delimit informative regions in which the evidence in favor of one of the competing models is larger than 10 (100) to 1. As a rule of thumb, odds of at least 10 : 1 are necessary for an informative statement, following previous literature on the subject (see e.g. Kass & Raftery 1995). It is apparent from Figure 12 that for moderately informative data ($I > 2$) the measured mean has to lie at least about 4 standard deviations away from β_0 in order to robustly disfavor the

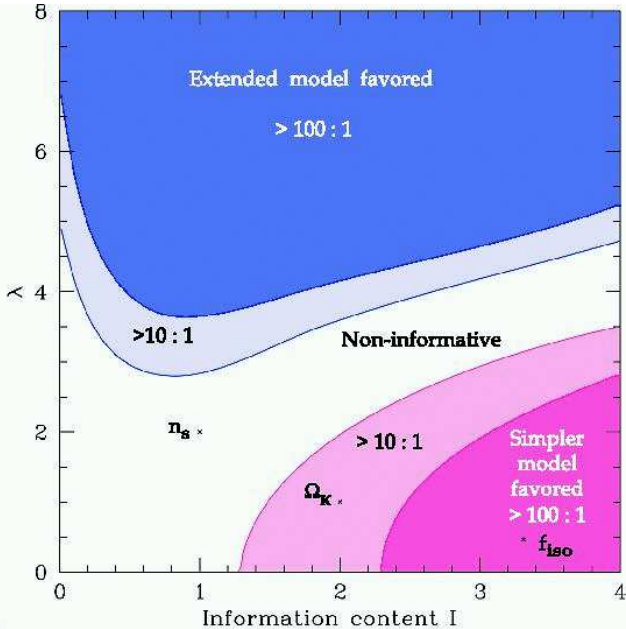


Figure 12. Informative regions (shaded) where one of the competing models has posterior odds larger than 10 (light shaded region) or 100 (dark shaded region) against 1. The white region corresponds to a non-informative limit. For this plot, we took advantage of the Savage-Dickey ratio assuming a Gaussian marginalized posterior for the parameter of interest and a Gaussian, separable prior. The location of the three parameters analyzed in the text in the $(I;)$ plane is shown by crosses.

simpler model (i.e., > 4). Conversely, for < 3 highly informative data ($I > 2$) do favor the conclusion that $! = !_0$. In general, a large information content favors the simpler model, because Occam's razor penalizes the large volume of "wasted" parameter space of the extended model. A large I disfavors exponentially the simpler model, in agreement with the sampling theory result. The location on the plane of the three cases discussed in the text (the scalar spectral index, the spatial curvature and the CDM isocurvature component) is marked by crosses in Figure 12. In each case we plot the most informative combination of data. Even though the informative regions of Figure 12 assume a perfect Gaussianity for the posterior marginalized pdf, they are illustrative of the results one might obtain in real cases, and can serve as a rough guide for the Bayes factor determination.

5.2 Validity of approximations

We have seen that the Laplace approximation and the Savage-Dickey formula can be used as handy tools for model comparison, sidestepping the need of carrying out a numerically demanding integration of the posterior over all parameter space. A completely satisfactory treatment would require the development of methods to estimate at the same time the error on the resulting Bayes factor. However, it seems less of a priority to achieve a high numerical precision in the Bayes factor, in view of the fact that model comparison results can strongly depend on the parameter space one assumes (as shown by the example of the isocurvature fraction). Therefore, fast methods to compute the Bayes factor,

such as the Savage-Dickey formula or the Laplace approximation, are very handy for exploring the consequences of a change of basis and the corresponding change of prior. Here we concisely comment on the validity of the approximations involved, keeping in mind that all we need is a precision less than unity in the log of the Bayes factor.

The Laplace approximation to the posterior volume, Eq. (22), fails in the case of heavily non-Gaussian distributions. To a certain extent, this pathology can be cured by going over to a set of "normal parameters", in which the posterior pdf is close to Gaussian and the parameters' directions uncorrelated. Usually, this new set of parameters has a physical interpretation in terms of the quantities probed by the observation. The advantage of the Laplace approximation is that it can be applied to compare two disconnected models, which could have in principle two totally different sets of parameters.

The Savage-Dickey density ratio, Eq. (35), is an exact expression for separable priors, which does not assume anything about the normality of the distribution and is completely equivalent to thermodynamic integration. The accuracy of the resulting Bayes factor depends only on the normalization of the marginalized pdf, whose precision is limited by the Monte Carlo sampling of parameter space. Several tests are available to check for good coverage and mixing of the Monte Carlo chains, and in particular one can run the Monte Carlo at an higher temperature to ensure that the tails of the distribution are appropriately sampled. It is important to keep in mind that the Savage-Dickey formula is restricted to the comparison of nested models.

As already mentioned, the ExPO technique assumes Gaussianity of the pdf at two levels, and therefore its validity is limited by the same arguments given above for the Laplace approximation. Further study is needed to improve on this assumption, and to apply the ExPO in the context of Bayesian experiment design.

5.3 About the prior and how to set it

Contrary to the case of inference problems, the prior available range is the key quantity for model comparison. The underpinnings of the prior choice can be found in our understanding of model-specific issues. In this work we have offered two simple examples of priors stemming from theoretical motivations: the prior on the scalar spectral index is a consequence of assuming slow-roll inflation while the prior on the spatial curvature comes from our knowledge that the Universe is not empty (and therefore the curvature must be smaller than 1) nor overclosed (or it would have recollapsed). This simple observations set the correct scale for the prior on Ω , which is of order unity. In general, it is enough to have an order of magnitude estimate of the a priori allowed range for the parameter of interest. In view of the fact that it is the logarithm of the evidence that matters, it is unimportant to refine the prior, once we are content that its order of magnitude is meaningful in the context of the model considered.

The situation is different for essentially scale-free parameters, such as the adiabatic and isocurvature amplitudes of our third application (see however Lazarides et al. (2004) for a case where model-theoretical considerations set the prior for the primordial curvature amplitude). In the absence

of strong model-specific motivations to limit the prior range, or in the context of phenomenological model building, we have demonstrated that a sensitivity analysis yields the a priori accessible parameter space to the instrument. From this point of view, the prior becomes a computable quantity which depends on our expectations on the quality of the data we will be able to gather (but of course not on the data themselves).

An important caveat is the dependence of the Bayes factor on the basis one adopts in parameter space. As illustrated by the case of the isocurvature amplitude, this is especially relevant for parameters which can vary over many orders of magnitudes. We put forward that the choice of the parameter basis can be guided by our physical insight of the model under scrutiny and our understanding of the observations. This principle would suggest that one should adopt *a priori* along "normal variables" or principal components, because those are directly probed by the data and usually can be interpreted in terms of physically relevant and meaningful quantities. A general principle of consistency can be invoked and coupled to a sensitivity analysis to select the most appropriate variable for cases where many apparently equivalent choices are present (for example, f_{iso} , or $\frac{P}{P'}$). We leave further exploration of this very relevant issue to a future publication.

6 CONCLUSIONS

We have demonstrated that Bayesian evidence allows one to attach quantitative statements to one's intuitive understanding of model complexity and presented two methods to compute the Bayes factor of two competing models, avoiding altogether the computationally intensive integration of the posterior. For nested models, the Savage-Dickey density ratio, Eq. (35), provides an off-the-shelf tool for the evaluation of the Bayes factor at no extra computational cost than the Monte Carlo sampling of the parameter space. The Laplace approximation, Eq. (25), can be used to compare non-nested models as well, but is accurate only for approximately Gaussian posteriors. We have argued that confidence intervals should be interpreted carefully, and in particular that Bayesian model selection reasoning should be used to decide whether the introduction of a parameter is warranted by data. The main strengths of the Bayesian approach are that it does consider the information content of the data and that it allows one to compare predictions of a model, instead of just disproving them as in the sampling theory approach. We have introduced a new statistical technique (ExPO) which, relying on our current status of knowledge and taking into account present-day uncertainties, produces forecasts for the probability distribution of the Bayes factor from future experiments. We have also shown that a sensitivity analysis can be employed to compute an observation-specific prior on a scale-free parameter such as the isocurvature fraction.

We have applied this Bayesian model selection point of view to three central ingredients of present-day cosmological model building. Regarding the spectral index of scalar perturbations, we found that while current data do not allow to draw a conclusion about the presence of a tilt, Planck is likely to disfavor a scale invariant index with odds of 100 : 1

or greater. We obtained a moderate evidence in favor of a Universe (about 14 : 1) but only if the Hubble parameter is measured independently or if Supernovae luminosity distance measurements are employed. Because of the fundamental geometrical degeneracy, the CMB alone will not be able to improve significantly on this evidence, unless supplemented by CMB-orthogonal determinations of the matter density or the Hubble parameter. Finally, purely adiabatic initial conditions are strongly preferred to a mixed model containing a totally (anti)correlated CDM isocurvature contribution (odds larger than 1000 : 1), on the grounds of an Occam's razor argument, that the prior available parameter space is much larger than the small surviving posterior volume. Planck has the potential to measure an isocurvature fraction of order 0.1 with high signal-to-noise, or else it will further strengthen the preference for purely adiabatic initial conditions, reaching odds of some 10^4 : 1.

We believe that model comparison tools offer complementary insight in what the data can tell us about the plausibility of theoretical speculations regarding cosmological parameters, and can provide useful guidance in the quest of a cosmological concordance model.

ACKNOWLEDGMENTS

It is a pleasure to thank Sam Leach for many enlightening discussions and for stimulating my interest in sensitivity analysis and experiment design. I am grateful to Chiara Caprini, Ruth Durrer, Martin Kunz and Julien Lesgourgues for comments and to Christophe Ringeval for help with the informatics. This work is supported by the Tomalla Foundation and by the Royal Astronomical Society through the Sir Norman Lockyer Fellowship. The use of the Meyrin cluster owned and operated by the University of Geneva is acknowledged.

REFERENCES

- Amendola L., Gordon C., Wands D., Sasaki M., 2002, Phys. Rev. Lett., 88, 211302
- Bassett B. A., 2004, preprint: astro-ph/0407201
- Bassett B. A., Corasaniti P. S., Kunz M., 2004, Astrophys. J., 617, L1
- Bassett B. A., Parkinson D., Nichol R. C., 2004, preprint: astro-ph/0409266
- Beltran M., Garcia-Bellido J., Lesgourgues J., Liddle A. R., Slosar A., 2005, preprint: astro-ph/0501477
- Beltran M., Garcia-Bellido J., Lesgourgues J., Riazuelo A., 2004, Phys. Rev., D 70, 103530
- Bennett C. L., et al., 2003, Astrophys. J. Suppl., 148, 1
- Bowen R., Hansen S. H., Melchiorri A., Silk J., Trotta R., 2002, Mon. Not. Roy. Astron. Soc., 334, 760
- Bucher M., Dunkley J., Ferreira P. G., Moodley K., Skordis C., 2004, Phys. Rev. Lett., 93, 081301
- Trotta R., Garcia-Bellido J., Lesgourgues J., Riazuelo A., 2003, Phys. Rev. Lett., 91, 171301
- Trotta R., Lesgourgues J., Pastor S., 2003, Phys. Rev., D 67, 123005
- Di Ciccio T., Wasserman L., 1997, J. Amer. Stat. Assoc., 92, 903

Dickey J.M., 1971, *Ann. Math. Stat.*, 42, 204

Dickinson C., et al., 2004, preprint: astro-ph/0402498

Efstathiou G., Bond J.R., 1999, *Mon. Not. Roy. Astron. Soc.*, 304, 75

Freedman W.L., et al., 2001, *Astrophys. J.*, 553, 47

Goldstein J.H., et al., 2003, *Astrophys. J.*, 599, 773

Goodwin C., Lewis A., 2003, *Phys. Rev. D* 67, 123513

Hannestad S., 2003, *JCAP*, 0305, 004

Hinshaw G., et al., 2003, *Astrophys. J. Suppl.*, 148, 135

Hobson M.P., Bridle S.L., Lahav O., 2002, *Mon. Not. Roy. Astron. Soc.*, 335, 377

Jaynes E., 2003, *Probability Theory. The logic of science*. Cambridge University Press, Cambridge, U.K.

Kass R., Raftery A., 1995, *J. Amer. Stat. Assoc.*, 90, 773

Knox L., 1995, *Phys. Rev. D* 52, 4307

Kosowsky A., Kamionkowski M., Jungman G., Spergel D.N., 1996, *Nucl. Phys. Proc. Suppl.*, 51B, 49

Kosowsky A., Miličević M., Jimenez R., 2002, *Phys. Rev. D* 66, 063007

Kurki-Suonio H., Muuhonen V., Valiviita J., 2004

Lazarides G., de Austra R., Trotta R., 2004, *Phys. Rev. D* 70, 123527

Lewis A., Bridle S., 2002, *Phys. Rev. D* 66, 103511

Liddle A.R., 2004, *Mon. Not. Roy. Astron. Soc.*

Lindley D., 1957, *Biometrika*, 44, 187

Loredo T.J., 2003, in *AIIP Conf. Proc. ed., Proceedings of 23rd Annual Conference on Bayesian Methods and Maximum Entropy in Science and Engineering*, Jackson Hole, Wyoming, 3-8 Aug 2003 'Bayesian adaptive exploration'. pp 330-346

Lyth D.H., Wanders D., 2003, *Phys. Rev. D* 68, 103516

MacKay D., 2003, *Information theory, inference, and learning algorithms*. Cambridge University Press, Cambridge, U.K.

Marshall P., Rajguru N., Slosar A., 2004, preprint: astro-ph/0412535

Melchiorri A., Riotto L.M., 2001, *New Astron. Rev.*, 45, 321

Moodley K., Bucher M., Dunkley J., Ferreira P.G., Skordis C., 2004, *Phys. Rev. D* 70, 103520

Pierpaoli E., 2003, *Mon. Not. Roy. Astron. Soc.*, 342, L63

Pierpaoli E., Garcia-Bellido J., BORGNI S., 1999, *JHEP*, 10, 015

Readhead A.C.S., et al., 2004, *Astrophys. J.*, 609, 498

Riess A.G., et al., 2004, *Astrophys. J.*, 607, 665

Rocha G., Trotta R., Martins C., Melchiorri A., Avelino P., Bean R., Viana P., 2004, *Mon. Not. Roy. Astron. Soc.*, 352, 20

Saini T.D., Weller J., Bridle S.L., 2004, *Mon. Not. Roy. Astron. Soc.*, 348, 603

Skilling J., 2004, 'Nested Sampling for General Bayesian Computation', unpublished, available from: <http://www.inference.phy.cam.ac.uk/bayesys/>

Tegmark M., et al., 2004a, *Astrophys. J.*, 606, 702

Tegmark M., et al., 2004b, *Phys. Rev. D* 69, 103501

Trotta R., 2004, PhD Thesis N. 3534, University of Geneva, Switzerland, June 2004

Trotta R., Durrer R., 2004, in Ru ni et al. eds, *Proceedings of the X Marcel Grossman Meeting*, 20-26 July 2003, Rio de Janeiro 'Testing the paradigm of adiabaticity'

Trotta R., Hansen S.H., 2004, *Phys. Rev. D* 69, 023509

Trotta R., Riazuelo A., Durrer R., 2001, *Phys. Rev. Lett.*, 87, 231301

Trotta R., Riazuelo A., Durrer R., 2003, *Phys. Rev. D* 67, 063520

Valiviita J., Muuhonen V., 2003, *Phys. Rev. Lett.*, 91, 131302

Verde L., et al., 2003, *Astrophys. J. Suppl.*, 148, 195

Verdinelli I., Wasserman L., 1995, *J. Amer. Stat. Assoc.*, 90, 614